

# ELLIPSES, CARDIoids, AND PENROSE TILES

**A. J. Reuben**

1606/5 Albert Road, Strathfield, NSW 2135, Australia

**A. G. Shannon**

KVB College of Visual Communication, 99 Mount Street  
North Sydney, NSW 2060, Australia

*(Submitted April 1996-Final Revision November 1996)*

## 1. INTRODUCTION

Many macroscopic properties in nature represent the response of a system to an applied disturbance. Such properties as electrical or thermal conductivity, magnetic permeability, and dielectric permittivity fall into this category. They can all be described by the same model of an induced flux produced by an applied field or potential gradient. In this study we shall present the solution to a problem in plane geometry involving cardioids and ellipses which has arisen in the study of the interaction of electromagnetic waves with matter.

A major area of research in the field of condensed matter physics is the optical response of composite materials. Moreover, recent advances in nanostructure technologies have generated particular interest in the physical properties of composite thin films [4]. Such structures are made up of an otherwise uniform thin film of one material into which are embedded shafts or cylinders of a different material. The film constituents can be chosen so as to obtain desired bulk properties. In practice, the major constituent is a dielectric material into which metal columnar inclusions are deposited. The optical properties of the metal-dielectric thin films can be intermediate between those of the metal and of the dielectric. These films also exhibit significant angular and spectral selectivity. The former feature has practical importance in the production of window coatings which minimize solar heating and glare while the latter feature is of use in solar collectors. Composite thin films have recently been analyzed mathematically by means of a conformal mapping technique [10]. A schematic diagram of the film microstructure for obliquely deposited circular cylindrical columns is shown in Figure 1.

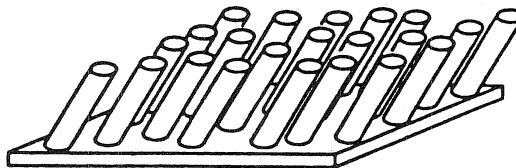


**FIGURE 1. Film Microstructure**

In general, the cylinder lengths are approximately equal to the film thickness. Therefore, by ignoring end effects such as fringing fields and restricting attention to a cross-section (normal to the cylinder axis), it becomes sufficient to model such a film as a plane figure. We therefore obtain a two-dimensional array of circles in the plane, each of which represents the cross-section of an individual cylindrical inclusion. During the production of the films it often happens that two

columns are deposited very close to each other and give the appearance of merging into one another. A mathematical model for this particular situation has recently appeared [9] which employs a symmetric pair of cardioids to describe the two-dimensional cross-section of the merging columns. During the analysis, the problem arose of determining the axis lengths of an ellipse of "best fit" enveloping the cardioid pair. The problem was solved and only the final numbers were presented. It was discovered that by choosing a suitable definition of best fit, the parameters of an optimal elliptical envelope for a cardioid pair could be determined exactly in terms of the *golden section*. We now present the full derivation of this interesting and unexpected result together with some concomitant findings that have been unearthed subsequently. An elliptical envelope for a pair of cardioids is shown in Figure 2.

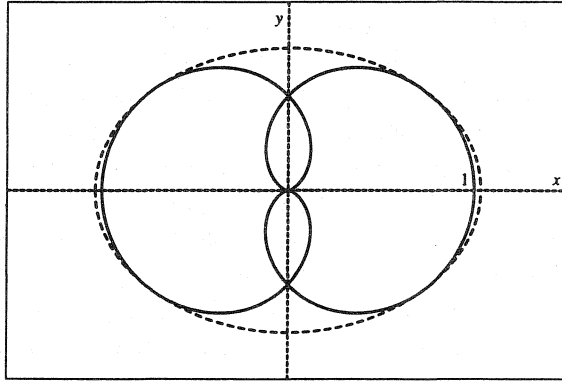


FIGURE 2. Cardioid Pair with Elliptical Envelope

## 2. GENERAL SCENARIO

The particular problem of interest can be considered as a special case of the following situation. We begin with the complex transformation

$$w_n = z^{-1/n} \quad (2.1)$$

in which  $w = u + iv$  and  $z = x + iy$ . If we consider contours in the (Cartesian)  $z$  plane defined by  $u = \text{Re}(w) = \text{constant}$  and set  $z = re^{i\theta}$ , we obtain

$$r = \cos^n(\theta/n) \quad (2.2)$$

as the contour in the  $z$  plane which is mapped onto the straight line  $u = 1$  in the  $w_n$  plane. When  $n = 1$  we have a circle of radius  $\frac{1}{2}$  centered at the Cartesian point  $(\frac{1}{2}, 0)$ . For  $n = 2$  we obtain a cardioid symmetric about the  $x$  axis whose equation may be written as

$$r = \frac{1}{2}(1 + \cos\theta). \quad (2.3)$$

By superimposing the closed curves given by (2.2) with their respective reflections in the  $y$  axis, we obtain pairs of intersecting contours. The conformal mappings (2.1) corresponding to  $n = 1$  and  $n = 2$  have been used to study the polarization response of touching [7], [8] and intersecting [9] particles, respectively. As  $n \rightarrow \infty$ , the degree of merging of the particle pair increases until, in

the limit, the contour corresponding to  $u = 1$  becomes the unit circle centered at the origin. In this paper we shall be considering elliptical envelopes for a pair of (left- and right-hand) cardioids (the  $n = 2$  case).

The approach to be adopted here will be to eliminate  $\theta$  and then ultimately express the ellipse area in terms of the radial coordinate of the point of tangency. Due to the symmetry of the cardioid pair with respect to both the  $x$  and the  $y$  axes, it will clearly be sufficient to work just within the first quadrant. Moreover, due to the shape of the cardioid pair, the horizontal axis of the desired optimal ellipse will be the major one. Hence, we can restrict attention to the right-hand cardioid in the first quadrant where  $0 \leq \theta \leq \pi/2$  and search for unrotated ellipses centered at the origin with horizontal and vertical semi-axis lengths of  $a$  and  $b$ , respectively, where  $a \geq b > 0$ .

The first step in determining our optimal ellipse is, naturally, to find the points of intersection of the relevant curves. In the general case, we must therefore begin by finding the points of intersection of the  $n$ -cardioid (2.2) and the ellipse. The polar equation of an ellipse with horizontal and vertical semi-axis lengths of  $a$  and  $b$ , respectively, is given by

$$r = \frac{ab}{\sqrt{a^2 + (b^2 - a^2) \cos^2 \theta}}, \quad a \neq 0 \neq b. \quad (2.4)$$

Eliminating  $\theta$  between (2.2) and (2.4) leads to the following polynomial equation for the value of the radial coordinate of the point(s) of intersection  $(\rho, \varphi)$ :

$$\rho^2 (T_n^2(\sqrt{\rho}) - \lambda - 1) + \mu = 0, \quad a \neq b, \quad (2.5)$$

where the functions  $T_n(s)$  are the Chebyshev polynomials of the first kind [11] and

$$\lambda = \frac{b^2}{a^2 - b^2}, \quad \mu = \frac{a^2 b^2}{a^2 - b^2}, \quad a \neq b,$$

which can be rearranged as

$$a = \sqrt{\frac{\mu}{\lambda}}, \quad b = \sqrt{\frac{\mu}{\lambda + 1}}. \quad (2.6)$$

In order that the solutions  $\rho$  represent points of tangency, we must also require that the slopes of the ellipse and the  $n$ -cardioid be the same at their point(s) of intersection  $(\rho, \varphi)$ . We can specify the slope of a curve at a given point by considering the angle  $\gamma$  between the tangent and radial vectors at that point. If we denote these angles for the ellipse and the  $n$ -cardioid by  $\gamma_E$  and  $\gamma_C$ , respectively, then the tangency condition at  $(\rho, \varphi)$  can be written

$$\tan \gamma_E = \tan \gamma_C, \quad (2.7)$$

where

$$\tan \gamma = \frac{rd\theta}{dr} = \frac{r(\theta)}{r'(\theta)}. \quad (2.8)$$

Substituting (2.2) and (2.4) into (2.7)-(2.8) yields, for  $a \neq b$ ,

$$\frac{\lambda + \sin^2 \varphi}{\sin 2\varphi} = \frac{1}{2} \cot\left(\frac{\varphi}{n}\right), \quad \varphi \neq 0, \pi/2,$$

or, by using (2.2) at  $(\rho, \varphi)$ :

$$\lambda + 1 = T_n^2(\rho^{1/n}) + \rho^{1/n} T_n(\rho^{1/n}) U_{n-1}(\rho^{1/n}), \quad \rho \neq 1, \quad (2.9)$$

where the  $U_n(s)$  are the Chebyshev polynomials of the second kind [11].

In the next section, we shall consider the interesting case of enveloping a pair of standard ( $n=2$ ) cardioids by an ellipse. In anticipation of the results to be obtained, we conclude this section by introducing the *golden section*,  $\tau = (1 + \sqrt{5})/2$ , a number also familiar as the positive solution to

$$x^2 - x - 1 = 0, \quad (2.10)$$

which is the characteristic equation for the sequence of Fibonacci numbers  $\{F_n\}$ . This sequence has many connections with the Chebyshev polynomials mentioned above [6], [11]. In addition, the identity

$$\frac{1}{m+n\tau} = \frac{m+n-n\tau}{m^2+mn-n^2}, \quad (2.11)$$

which is well known from the field  $\mathbb{Q}(\sqrt{5})$ , will be found useful in later sections.

### 3. THE ELLIPSE

We shall define an optimal elliptical envelope (or ellipse of best fit) to be an ellipse of *minimal area* which is tangent to and completely contains the cardioid pair. This provides precisely the right number of conditions necessary to determine the three key parameters: the value of the radial coordinate of the point of tangency,  $r = \rho$ , and the semi-axis lengths  $a$  and  $b$  of the desired ellipse. We will solve the problem in terms of  $\rho$  and then substitute back to find the required ellipse dimensions.

The first condition is that the cardioid and the ellipse must intersect. For  $a \neq b$  this is just (2.5) with  $n=2$ , which leads to the following equation for  $\rho$ :

$$\mu = \lambda\rho^2 + 4\rho^3 - 4\rho^4. \quad (3.1)$$

The second condition is the tangency requirement which is (2.9) with  $n=2$ . This yields

$$\lambda = 2\rho(4\rho - 3). \quad (3.2)$$

We now obtain an expression for  $\mu$  in terms of  $\rho$  by substituting (3.2) into (3.1) to find that

$$\mu = 2\rho^3(2\rho - 1). \quad (3.3)$$

Substitution into (2.6) of the respective expressions (3.2) and (3.3) for  $\lambda$  and  $\mu$ , together with some subsequent simplification, leads to:

$$a = \rho \sqrt{\frac{2\rho-1}{4\rho-3}}, \quad b = \rho \sqrt{\frac{2\rho}{4\rho-1}}, \quad \rho \neq 1/4, 3/4. \quad (3.4)$$

The expression for the area of an ellipse tangent to the cardioid pair in terms of  $\rho$  then follows directly from (3.4):

$$A(\rho) = \frac{\pi}{2} \rho^2 \sqrt{\frac{\rho(\rho-1/2)}{(\rho-3/4)(\rho-1/4)}}, \quad \rho \neq 1/4, 3/4. \quad (3.5)$$

Expression (3.5) for the ellipse area is defined only when  $\rho = 0$ ,  $1/4 < \rho \leq 1/2$  or  $3/4 < \rho \leq 1$ . In other words, an ellipse intersecting the cardioid at a point  $(\rho, \varphi)$  at which both curves have the same slope is only possible for  $\rho$  values in the above intervals. The graph of the ellipse area  $A(\rho)$  for  $0 \leq \rho \leq 1$  is plotted in Figure 3.

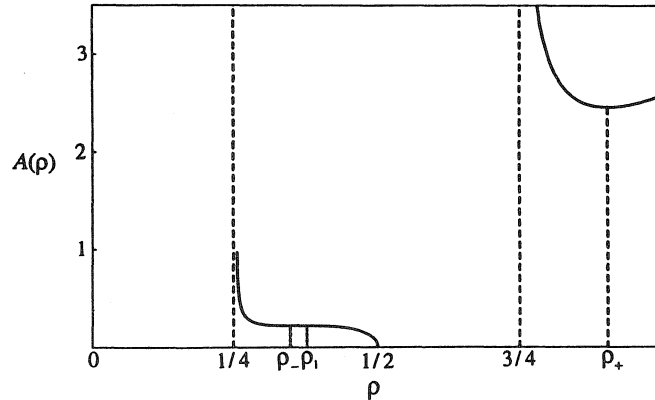


FIGURE 3. Graph of Ellipse Area

We can examine the meaning of these permissible intervals by considering what sort of ellipse will appear as the point of tangency moves along the right-hand cardioid. For the point  $P(1, 0)$  we have  $\rho = 1$  and, by (3.4), obtain an ellipse with  $a = 1$  (as expected) and  $b = \sqrt{2/3}$ . As our point moves (in the positive  $\theta$  sense) along the cardioid, the  $\rho$  value decreases from unity and we approach the point of maximum vertical elevation. At this point, the tangent to the cardioid is horizontal and so the touching ellipse in this case will have an infinitely long horizontal axis and its area will be undefined. This point corresponds to  $\rho = 3/4$  and so, from (3.4), we see that  $a$  is undefined (as expected) and that  $b = 3\sqrt{3/8}$ .

Before completing the problem, we pause briefly to dispose of the two cases not encompassed in the above derivation. These are the cases for which  $a = b$  and  $\rho = 1$  ( $\varphi = 0$ ). In the former case, the point of intersection is  $P(1, 0)$  and the covering ellipse reduces to the unit circle centered at the origin. In the latter case, we obtain ellipses for which  $b < a = 1$ . All such ellipses share a common vertical tangent with the cardioid at the point  $P$ , where their curvature is given by  $1/b^2$ . At  $P$  the cardioid has a curvature equal to  $3/2$  [12]. Only those ellipses whose curvature at  $P$  is less than  $3/2$  will lie completely outside the cardioid. Hence, we must have  $b^2 \geq 2/3$ . The ellipse of least area satisfying this condition,  $E$  say, is obviously the one for which  $b = \sqrt{2/3}$ . The generic expressions (3.4) therefore reproduce this result for the  $\rho = 1$  case. In fact, the tangency condition (3.2) implies that the solutions  $\rho$  are double roots of (3.1), and  $\rho = 1$  is indeed such a double root for  $a = 1$  ( $\lambda = \mu$ ) precisely when  $b = \sqrt{2/3}$ .

#### 4. GENERIC SOLUTION

The final stage of the generic solution is to determine the geometrically reasonable ( $\rho > 0$ ) critical points of the area function  $A(\rho)$ . The third condition is therefore the choosing of those  $\rho$  values for which the derivative  $A'(\rho)$  becomes zero. By imposing this requirement, we will find the  $\rho$  value corresponding to the outer elliptical envelope of minimal area—that is, the optimal ellipse. However, due to the nature of this approach, in determining the critical points of  $A(\rho)$  we shall find *another* tangent ellipse whose dimensions will also be of interest.

Differentiating the square of (3.5) with respect to  $\rho$ , simplifying, and then setting the result to zero, leads to the equation  $\rho^4 g(\rho) = 0$ , where

$$g(\rho) = 128\rho^3 - 208\rho^2 + 100\rho - 15. \quad (4.1)$$

The solutions of interest will naturally come from the zeros of the cubic polynomial  $g(\rho)$  defined in (4.1). As we now show, these can all be determined exactly.

As  $g(1)$  is nonzero and  $0 < \rho \leq 1$ , there will be no integer solutions for  $g(\rho) = 0$  (excluding the trivial case). Therefore, since the coefficients of  $g(\rho)$  are all integral, any rational solutions will have the form  $p/q$ , where  $p|15$ ,  $q|128$ , and  $p < q$  [1]. The only nontrivial rational zero of  $g(\rho)$  is found to be  $\rho_1 = 3/8$ . This leads to the factorization

$$g(\rho) = (8\rho - 3)(16\rho^2 - 20\rho + 5). \quad (4.2)$$

The remaining critical points are the zeros of the quadratic factor on the right-hand side of (4.2). These can be written as

$$\rho_+ = \frac{1}{4}(2 + \tau), \quad \rho_- = \frac{1}{4}(3 - \tau). \quad (4.3)$$

By considering the sign of the second derivative of  $A(\rho)$  (or otherwise), it is readily seen that the rational solution  $\rho_1$  corresponds to a local maximum for the area of the tangent ellipse while the remaining two conjugate solutions  $\rho_{\pm}$  correspond to local minima for this area. This is also clear from the graph of  $A(\rho)$  displayed in Figure 3. We shall denote by  $E_{\pm}$  the ellipses corresponding to  $\rho_{\pm}$ , respectively. The larger of the two (conjugate) ellipses,  $E_+$ , is the desired unique optimal ellipse completely enclosing the cardioid pair. Its area is less than that of the two additional plane figures considered separately above, namely, the unit circle and the ellipse  $E$ .

The semi-axis lengths of the ellipse  $E_+$  and the angular coordinate  $\varphi_+$  of its point of intersection  $P_+$  with the right-hand cardioid are found by substituting  $\rho_+$  into (3.4) and (2.3), respectively. With the aid of (2.11) and the fact that  $\tau$  satisfies (2.10), we obtain

$$a_+ = \frac{1}{4\sqrt{2}}(1 + 3\tau), \quad b_+ = \frac{\sqrt{5}}{4\sqrt{2}}\sqrt{2 + \tau}, \quad (4.4)$$

and

$$\cos \varphi_+ = \frac{\tau}{2}, \quad (4.5)$$

or just (see [2])  $\varphi_+ = \pi/5$ . We can immediately determine the focus  $F_+$  and eccentricity  $e_+$  of  $E_+$  from (4.4):

$$F_+ = \frac{\sqrt{5}}{4}\sqrt{\tau}, \quad e_+ = \sqrt{2(2\tau - 3)}. \quad (4.6)$$

The relative area excess of  $E_+$  over the double cardioid,  $DC$ , turns out to be

$$\frac{A_{E_+} - A_{DC}}{A_{DC}} = a_+ b_+ / (3/8 + 1/\pi) - 1 \approx .1223.$$

### 5. CONJUGACY RELATIONS

There is a whole series of interesting relations linking the dimensions of the two conjugate ellipses  $E_{\pm}$ . In these last two sections we present this material together with some related geometric constructions. We therefore begin by considering the tangent ellipse  $E_-$  and implicitly drop the restriction that  $0 \leq \theta \leq \pi/2$ . By substituting  $\rho_-$  into (3.4) and (2.3) and again using (2.10) and (2.11), we obtain the following semi-axis lengths for  $E_-$ :

$$a_- = \frac{1}{4\sqrt{2}}(3\tau - 4), \quad b_- = \frac{\sqrt{5}}{4\sqrt{2}}\sqrt{3 - \tau}, \tag{5.1}$$

and the following angular coordinate  $\varphi_-$  for the point of intersection  $P_-$  of  $E_-$  with the right-hand cardioid:

$$\cos \varphi_- = -\frac{1}{2}(\tau - 1), \tag{5.2}$$

or just (see [2])  $\varphi_- = 3\pi/5$ . The focus  $F_-$  and eccentricity  $e_-$  of  $E_-$  follow from (5.1):

$$F_- = \frac{\sqrt{5}}{4}\sqrt{\tau - 1}, \quad e_- = \sqrt{\frac{2}{5}}\sqrt{2\tau - 1}. \tag{5.3}$$

The ellipse  $E_-$  has its major axis lying along the  $y$  axis and actually *cuts* both cardioids. However, this ellipse can still be said to be tangential to the cardioid since, at the point of intersection, the curves have the same slope. In Figure 4 the two ellipses  $E_{\pm}$  are shown superimposed onto the right-hand cardioid. We also make note of the angle  $\varphi_1$  which corresponds to the rational zero  $\rho_1$  of (4.1) and which, by (2.3), satisfies

$$\cos \varphi_1 = -\frac{1}{4}. \tag{5.4}$$

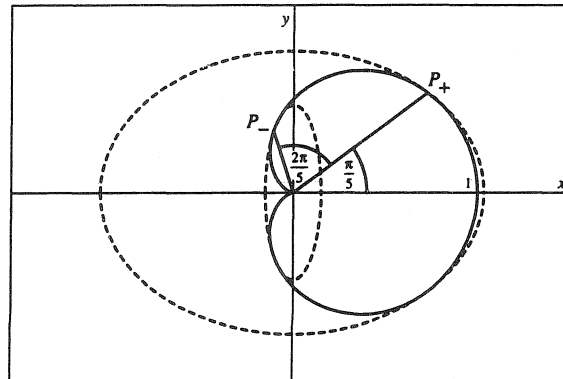


FIGURE 4. Right-Hand Cardioid with Conjugate Ellipses

In the following, we list several conjugacy results based on the values of the various ellipse parameters. Identities (2.10) and (2.11) for  $\tau$  have been used where convenient to simplify the working.

Straightforward calculations employing (4.6) and (5.3) and then (4.5), (5.2), and (5.4) lead to

$$\frac{F_+}{F_-} = \tau, \quad \frac{1}{e_+^2} - \frac{1}{e_-^2} = 1, \quad \text{and} \quad \cos \varphi_+ \cos \varphi_- = \cos \varphi_1.$$

Using (4.4) and (5.1), it can also be shown that

$$\frac{1}{2} \left( 1 + \frac{b_+ b_-}{a_+ a_-} \right) = \tau = \frac{1}{2} \left( \frac{a_+ b_-}{a_- b_+} - 1 \right),$$

from which one immediately obtains

$$\frac{1}{4} \left( \frac{a_+ b_-}{a_- b_+} + \frac{b_+ b_-}{a_+ a_-} \right) = \tau.$$

By considering the ratios of corresponding quantities for the two conjugate ellipses  $E_{\pm}$ , it can be shown that the following set of quotients are all equal to  $\tau$ :

$$\tau = \frac{b_+}{b_-} = \sqrt[5]{\frac{A_+}{A_-}} = \sqrt[4]{\frac{a_+}{a_-}} = \sqrt{\frac{\rho_+}{\rho_-}} = \sqrt[4]{\frac{x_+}{x_-}} = \frac{y_+}{y_-},$$

where the  $A_{\pm}$  are the areas of the respective conjugate ellipses and the lengths  $x_{\pm}$  and  $y_{\pm}$  denote the Cartesian coordinates of the corresponding points  $P_{\pm}$ .

Another interesting result involves arc lengths along the (right-hand) cardioid. The expression for the arc length along the cardioid (2.3) from the point  $P(1, 0)$  is  $s(\theta) = 2 \sin(\theta/2)$  (see [12]). At the points  $P_{\pm}$  we therefore obtain

$$s(\varphi_+) = 2 \sin \frac{\varphi_+}{2} = \tau - 1, \quad s(\varphi_-) = 2 \sin \frac{\varphi_-}{2} = \tau,$$

where we have used (4.5) and (5.2). The arc length along the cardioid from  $P_+$  to  $P_-$  is thus precisely one unit.

We can also consider curvatures. The curvature of the ellipse (2.4) at a point  $(r, \theta)$  is given by (see [12])

$$K(r, \theta) = \frac{a^4 b}{(a^4 + (b^2 - a^2)r^2 \cos^2 \theta)^{3/2}}. \quad (5.5)$$

Substituting the polar coordinates of the points  $P_{\pm}$  into (5.5), using (4.4) and (5.1), and then taking the resulting ratio, leads to

$$\frac{K_+}{K_-} = \tau, \quad (5.6)$$

where the  $K_{\pm}$  denote the curvatures of the ellipses  $E_{\pm}$  at their respective points of intersection  $P_{\pm}$  with the right-hand cardioid. A result analogous to (5.6) can also be shown to hold for the ratio of the curvatures of the right-hand cardioid at the points  $P_{\pm}$ .

6. PENROSE TILES

A routine calculation reveals that the slope of the tangent line at  $P_+$  is equal to  $\tan 4\pi/5$ . By drawing in that part of this tangent line which lies in the first quadrant and then repeating the analogous procedure in the other three quadrants, we obtain a rhombus  $R$  with angles of  $2\pi/5$  on the  $x$  axis and angles of  $3\pi/5$  on the  $y$  axis. This quadrilateral is in fact known as a *Penrose rhombus* because it can be divided up to form two *Penrose tiles* [5]. This is shown in Figure 5. The two Penrose tiles with colored vertices (which do not concern us here) have been dubbed *darts* and *kites* (after John Horton Conway) [3]. The partition  $BGD$  (where  $\angle BGD = 4\pi/5$ ) divides  $R$  into the dart  $BCDG$  and the kite  $ABGD$ . Using some simple trigonometry, it can be shown that the length of  $OG$  is in fact equal to  $\rho_-$ . Also, the partitions formed by the rays  $OP_+$  and  $OP'_+$  form another Penrose rhombus  $OP_+AP'_+$  which is one-quarter the size of  $R$ . Some elementary algebra also reveals that  $E_+$  is in fact the ellipse of greatest area that can be inscribed within  $R$ .

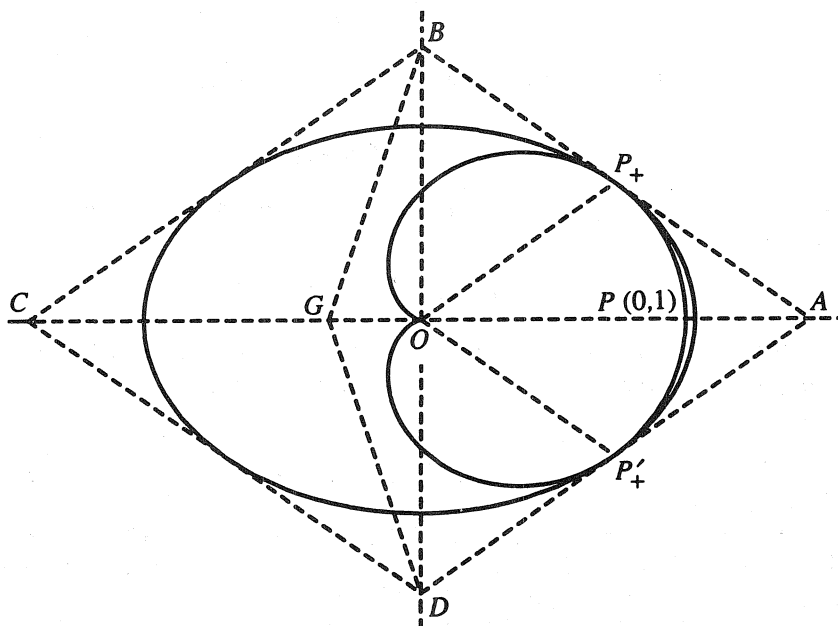


FIGURE 5. Right-hand Cardioid and Optimal Ellipse with Penrose Rhombus Divided into a Dart and a Kite

Another construction highlights the relationship between the darts and kites and the intersection points. It is possible to use intervals through these points to form new darts and kites. The upper and lower points of intersection of  $E_-$  with the left-hand cardioid will be denoted  $Q_-$  and  $Q'_-$ , respectively. We first produce both  $CB$  and  $OQ_-$  until they meet at  $H$  and then do the same with both  $CD$  and  $OQ'_-$  and the point  $I$ . In this way we form the dart  $OHCI$ . The contiguous quadrilateral  $AB'OD'$  then turns out to be a kite. These structures are displayed in Figure 6. After some elementary geometric considerations, it can be shown that the ratio of the area of the dart  $OHCI$  to that of the kite  $AB'OD'$  is precisely equal to the golden section,  $\tau$ .

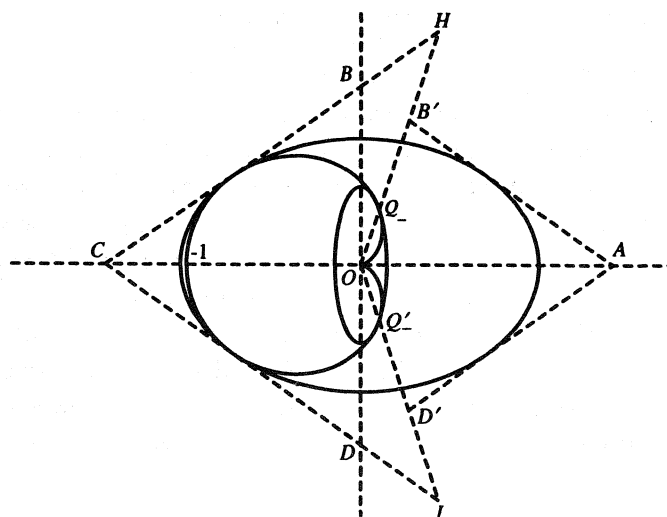


FIGURE 6. Additional Darts and Kites

#### ACKNOWLEDGMENT

The authors would like to express their gratitude to the anonymous referee for many thoughtful and valuable suggestions.

#### REFERENCES

1. G. Birkhoff & S. MacLane. *A Survey of Modern Algebra*. New York: Macmillan, 1953.
2. H. M. Cundy & A. P. Rollett. *Mathematical Models*. Oxford: Oxford University Press, 1961.
3. M. Gardner. *Penrose Tiles to Trapdoor Ciphers*. New York: W. H. Freeman, 1989.
4. C. G. Granqvist, ed. *Materials Science for Solar Energy Conversion Systems*. Oxford: Pergamon Press, 1991.
5. B. Grünbaum & G. C. Shephard. *Tilings and Patterns*. New York: W. H. Freeman, 1987.
6. A. F. Horadam. "Tschebyscheff and Other Functions Associated with the Sequence  $w_n(a, b; p, q)$ ." *The Fibonacci Quarterly* **7.1** (1969):14-22.
7. R. C. McPhedran & W. T. Perrins. "Electrostatic and Optical Resonances of Cylinder Pairs." *Applied Physics* **24** (1981):311-18.
8. A. V. Radchik, G. B. Smith, & A. J. Reuben. "Quasistatic Optical Response of Separate, Touching, and Intersecting Cylinder Pairs." *Physical Review B* **46** (1992):6115-25.
9. A. V. Radchik, A. V. Paley, & G. B. Smith. "'Invisibility' in Certain Intersecting Particles and Arrays of Such Particles in a Solid Host." *J. Applied Physics* **79.5** (1996):2613-21.
10. A. J. Reuben, A. V. Radchik, & G. B. Smith. "The Polarizability of Cylinder Arrays in Two Dimensions." *Annals of Physics* **242.1** (1995):52-76.
11. Th. J. Rivlin. *The Chebyshev Polynomials*. 2nd ed. New York: Wiley-Interscience, 1974.
12. M. Vygodsky. *Mathematical Handbook*. Moscow: Mir Publishers, 1975.

AMS Classification Numbers: 11B39, 78A05

